Accepted Manuscript

Title: Structure-reactivity relationship in pyrolysis of plastics.
A comparison with natural polymers

Authors: T. Larraín, M. Carrier, L.R. Radovic

PII: S0165-2370(17)30078-5
DOI: http://dx.doi.org/doi:10.1016/j.jaap.2017.05.011
Reference: JAAP 4041

To appear in: *J. Anal. Appl. Pyrolysis*

Received date: 17-1-2017
Revised date: 16-4-2017
Accepted date: 19-5-2017

Please cite this article as: T.Larraín, M.Carrier, L.R.Radovic, Structure-reactivity relationship in pyrolysis of plastics.A comparison with natural polymers, Journal of Analytical and Applied Pyrolysishttp://dx.doi.org/10.1016/j.jaap.2017.05.011

Structure-reactivity relationship in pyrolysis of plastics.
A comparison with natural polymers

T. Larraín[1,2], M. Carrier[3,*] and L. R. Radovic[1,2,4,*]

[1] Unidad de Desarrollo Tecnológico (UDT), University of Concepción, Chile

[2] Department of Chemical Engineering, University of Concepción, Chile

[3] European Bioenergy Research Institute, Aston University, UK

[4] Department of Energy & Mineral Engineering, Penn State University, USA

* to whom correspondence should be sent (m.carrier@aston.ac.uk or lrr3@psu.edu)

Highlights

- Global activation energy depends on conversion in pyrolysis of all polymers.
- Activation energy variability is proportional to chemical complexity of polymers.
- An Evans-Polanyi relationship for initiation reactions of polymer pyrolysis is proposed.

Abstract

Recent advances in plastics recycling confirm the high potential of pyrolysis technologies to enhance recovery and selectivity rates. Modelling the kinetics of this complex process to stimulate scaling-up opportunities remains a major challenge.This study is an attempt to develop practical quantitative reactivity indices for the pyrolysis of natural and synthetic polymers. Representative samples from both categories (coal and pine *vs.* PET, PE and PMMA) were selected. Their weight loss during pyrolysis was determined experimentally and analyzed using judicious lumping procedures for its initiation, propagation and termination steps. The combined experimental and theoretical approach allowed us to determine apparent activation energies using the isoconversional Friedman method; and the use of Benson's group contribution method generated reaction enthalpies for the initiation reactions. Increasing activation energies with conversion in each case indicated that bond scission proceeds in order of increasing bond strength. The greater chemical complexity of natural polymers was reflected in the higher coefficients of variability for activation energy and wider ranges of reaction enthalpies. A structure-reactivity relationship based on the Evans-Polanyi theory was used to test the hypothesis that primary pyrolysis kinetics is controlled by cleavage of weakest chemical bonds. While the results show that this approach is promising, especially if confirmed by extension to a larger data set, they also suggest the need to compare the relative kinetic importance of initiation and propagation steps in the sequence of polymer pyrolysis reactions.

Keywords: pyrolysis, polymers, kinetics, thermodynamics, Evans-Polanyi.

1. Introduction

The global production of plastics has grown *ca.* 9% per year between 1950 and 2012, and the generation of plastic waste has followed suit [1]. All the economic indicators suggest that this situation will continue [2]. Approximately half of the consumption is in the single- and short-term-use packaging sectors (*e.g.*, 40% in the EU [1] and 44% in Japan [3]). Such unsustainable accumulation of municipal and industrial waste in both developed and developing nations offers clear incentives to improve existing and propose new plastics recycling technologies.The economic incentives are equally compelling. In the face of increasing societal concerns for the environment and public health [4], plastic waste is emerging as priority recycling material, in order to avoid the use of landfills and other increasingly expensive (and/or inconvenient) disposal methods.

Mechanical recycling is currently the most common option – *e.g.*, 25% in the EU [3] and 22% in Japan [4]) – and the Plastic Industry Trade Association has developed recycling codes in an attempt to facilitate this process; but it is becoming quite expensive in the increasingly prevalent case of mixed complex waste (containing excessively dirty and/or diverse classes of plastic materials). At the other extreme, incineration and other forms of energy recovery may not be environmentally acceptable (*e.g.*, due to emissions of dioxins). Therefore chemical recycling emerges as the best option to process a complex mixture of these mostly organic feedstocks. And among the various processes within feedstock recycling, some of which are more appropriate for conversion to energy or fuels (*e.g.*, gasification, blast-furnace reduction), pyrolysis seems the best option: it is flexible and offers numerous operational and environmental advantages and financial benefits [5]. Thus, an in-depth understanding of thermal treatment of plastics is increasingly important as well.

Here the main challenge is a judicious kinetic analysis of its many parallel and consecutive molecular-scale reactions. Extensive and continuous efforts made in this field since the 1950s have been documented in the abundant literature. For example, after methodically collating information on the pyrolysis of polyethylene (PE), Poutsma added that "kinetic and product data for pyrolysis of molten PE are voluminous but inconsistent" [6]; and Kannan *et al.* (2014) [7] concluded that "a literature review conducted on the kinetics of LDPE pyrolysis has revealed significant discrepancies within kinetic parameters". In fact, Poutsma [8] demonstrated that the absence of a rigorous analytical methodology and of reaction regime control could lead to contradicting mechanistic interpretations. Similar inconsistencies have also been reported elsewhere for polyisobutylene [9], polystyrene (PS) [8] and biomass [10,11]. Such contradictions have obvious implications for technological progress in terms of reactor design.

A number of experimental and data treatment issues have been reported that could explain such contradictions. For example, a thermal lag produced by the difference between measured and sample temperatures leads to the ubiquitous compensation effect [12,13]. Also, virtual elimination of heat and mass transfer limitations (such that the Biot number is less than 0.1) is crucial for a reliable methodology, even though many authors do not take it into account. Regarding these issues, the Kinetics Committee of the International Confederation for Thermal Analysis and Calorimetry (ICTAC) [14] recommends a very useful step-by-step methodology: (i) “obtain quality kinetic data at no less than three different temperature programs”, (ii) “apply an isoconversional method (obtaining the E_α vs. α dependence is by itself sufficient for making kinetic predictions)”, (iii) “evaluate the whole kinetic triplets [model, reaction order and activation energy] by linear or non-linear model fitting with a cautious selection of the model”, and (iv) “validate the computed kinetic parameters by demonstrating that they can be used to satisfactorily predict (reproduce) the experimental kinetic curves from which these parameters have been computed.”

In an attempt to provide reliable kinetic parameters for complex chemical reactions, researchers have extensively used isoconversional methods; they offer the possibility of describing their temperature dependence using the isoconversional rates without assuming a specific reaction model [14]. Isoconversional methods assume that the reaction rate is temperature-dependent only at constant conversion (α); using multiple heating programs (*e.g.*, different heating rates) such a method can describe the process in a wide temperature range and “has been used broadly and fruitfully because it presents a fortunate compromise between the single-step Arrhenius kinetic treatments and the prevalent occurrence of processes whose kinetics are multi-step and/or non-Arrhenius” [15]. Thus, for example, Vyazovkin argued that both the variability of the frequency factor (A) and the ambiguity in interpreting the best-fit mathematical function (f(α)) lead to the conclusion that “the most informative part of the triplet [A, f(α) and Eα] appears to be the experimental value of Eα” [16].

Friedman’s method [17] has been very useful to determine variations of Eα with conversion and is therefore appropriate for comparison of pyrolysis profiles of different polymers. According to the transition state theory, the value of Eα in a chemical regime is a function of the activation energy of the individual steps and its value is determined by contributions of the individual steps to the overall reaction rate. A typical example is a distribution of activation energies for different plastics that represent the threshold of homolytic scission of weak bonds [15,18]. As in the pyrolysis of simple hydrocarbons [19], it is tempting to explore whether such reactions also represent the limiting steps in the pyrolysis of complex materials.

In concert with such an experimental approach, the application of a theoretical analysis that explores correlations between structure and reactivity is of interest when comparing reactivities of polymers. In this context, the Evans-Polanyi principle ($E = E_0 + x \cdot \Delta H_{rxn}$) has often been used for this purpose. When x ≈ 1, the transition state is product-like (*e.g.*, in homolytic scission); when x ≈ 0, the transition state is reactant-like.

To the best of our knowledge, this principle has not been used to compare pyrolysis reactivities of different polymers. Indeed, if homolytic scission is one of the primary degradation modes for different polymers, a correlation may be expected between the activation energy and the enthalpy of initiation reactions, even upon decomposition of these admittedly complex materials. Thus, for example, methane combustion is much slower than that of C_2^+ alkanes because of the difference in C-H vs C-C bond dissociation energies. Hence, this principle should offer additional molecular-level insights for comparison and better understanding of polymer pyrolysis. The main goal of this study was to seek a mechanistic understanding of the similarities and differences in pyrolysis reactivity of natural and synthetic polymers. This includes a relationship between simple but meaningful kinetic parameters and selected thermodynamic properties based on their well known differences in chemical structure.

2. Materials and Methods

2.1 Materials preparation and characterization

Polymethyl methacrylate (PMMA, MW~15,000), polyethylene (PE) with an average molecular weight of 35,000 g/mol and a density of 0.906 g/mL at 25°C, and polyethylene terephthalate (PET) reinforced with 30 wt% glass were purchased from Sigma-Aldrich. They were milled in a microfine grinder (IKA MF-10 basic). The pine sample was obtained from Unidad de Desarrollo Tecnológico (UDT) at the University of Concepción and milled in an analytical mill (IKA A11 basic). Particles < 106 µm were used in the pyrolysis experiments. A sub-bituminous coal sample was obtained from the Carbocat Laboratory at the University of Concepción and reduced to < 73.5 µm using a ball mill (model Pulverisette 6 from Fritsch).

Ultimate analysis (C, H, N, S - O) was performed in accordance with the ASTM D5016 standard method using a Leco TruSpec 2.5x apparatus; oxygen content was determined by difference. Moisture and ash contents were obtained according to ASTM E871-82 (2013) and ASTM E1755-01 (2015), respectively. The results of this analysis are shown in Table 1. The C/H and C/O ratios coincide with the theoretical molar ratios for PMMA (7.2 and 2.3), PE (0.5 and C/O is not applicable) and PET (12.0 and 1.9) and the agreement with literature values for pine [20,21] and sub-bituminous coal [22–25] is satisfactory. The presence of sulfur, oxygen and nitrogen in PMMA is attributed to the use of polymerization agents (persulfate salts, peroxides or azo compounds) [26,27].

2.2 Kinetic analysis

Fixed-bed pyrolysis experiments were conducted using thermogravimetric analysis (TGA - Pyris 1, PerkinElmer) in the atmosphere of ultra high purity N_2 at 50 mL/min. Samples of PMMA, PE or PET (11±1 mg) and pine or coal (5±1 mg) were weighed in a Sartorius microbalance (ME36S model) and loaded in a ceramic pan (7 mm in diameter, 2 mm deep; approx. 66 µL). The synthetic polymer samples were heated from room temperature to 700 ºC using low heating rates (5, 10, 20 and 50 °C/min). A different heating progam was used for the natural polymers to ensure their complete devolatilization: from room temperature to 105 °C at 15 °C/min followed by an isothermal stage at 105 °C for 45 min, then heated again from 105 to 900 °C at 5, 10, 20 and 50 °C/min, and finally maintained at 900 °C for 20 min.

The iso-conversional (Friedman's) method was selected for data analysis [17]. Non-isothermal and heterogeneous reactions are conveniently described by the following mass-based equations:

$$\frac{d\alpha}{dt} = k(T) \cdot f(\alpha) = A \cdot \exp\left(\frac{-E_A}{RT}\right) \cdot f(\alpha) \tag{1}$$

with

$$\alpha = \frac{m_i - m}{m_i - m_f}\,, \tag{2}$$

where α is the extent of reaction (conversion), A is the pre-exponential factor, E_α is the apparent activation energy, m_i is the initial mass of reactant, m is its mass at a certain time during the reaction, m_f is the final mass at the end of reaction. The function f(α) embodies the kinetic model (e.g., reaction-order model) and implicitly recognizes that the rate constant is a function of both temperature and conversion [15]. The MATLAB software was used to extract kinetic parameters using the methodology described elsewhere [28] and summarized in Figure 1. It consisted in two steps: (1) data processing with removal of dehydration stage, normalization of data, determination and smoothing of conversion, derivation of conversion, as well as removal of all negative and null data; and (2) determination of apparent activation energy at each conversion level (between 0.06 and 0.95 in 0.01 intervals) following Friedman's method. Only data obtained with a correlation coefficient above 0.9 – at 95% confidence – were analyzed further.

2.3 Calculation of reaction enthalpy

The group contribution method of Benson was used to calculate the enthalpy of dissociation of the principal bonds present in each polymer. The step-by-step methodology is also summarized in Figure 1. The bond dissociation equations were defined for each case (see Table S3): end-chain scission and random scission for plastics, and cleavage of weak bonds in coal or pine [29,30]. The enthalpies of formation were calculated using Benson's method [31–33] and databases provided by Domalsky *et al.* [34], Poutsma [35] and Zakarian [36].

3. Results and Discussion

3.1 Pyrolysis profiles

When exposed to pyrolysis conditions, different polymers exhibit large differences in their weight loss. Figure 2 shows the integral and derivative curves obtained at 10 °C/min and

Table 2 summarizes the key pyrolysis characteristics of each polymer studied. The presence and extent of early decomposition of natural polymers is due to their dehydration, which is non-existent in plastics; this result is in accordance with their measured moisture content that is highest in coal (Table 1). Synthetic polymers decompose in one or two steps and in a more narrow temperature range, while natural polymers undergo further and different degradation stages over a wide range of temperatures. Synthetic polymers also decompose by virtue of a rapid depolymerization process with maximum rates of 10.8, 21.1 and 26.1 wt%/min for PET, PMMA and , PE; this is in contrast to pine (10.2 wt.%/min) and coal (1.8 wt%/min).

The decidedly less complex pyrolysis profile of synthetic polymers is in accordance with the description of degradation schemes available in the literature. Thus, for example, during pyrolysis of our PMMA sample the initial degradation (between 133 and 275 °C) led to 5 wt% material loss whereas the main decomposition step (between 275 and 430 °C) was responsible for 94 wt%. It is well established that PMMA decomposes predominantly to the monomer, MMA, through unzipping reactions such as end-chain beta-scission or end-chain depolymerization [37–42]. As a result, the first stage could be attributed to breakdown of weak bonds at lower temperature through random scissions while the second involves mainly end-chain reactions; this confims the dominant mechanism of unizipping at intermediate and high temperatures. It should also be noted that the different degradation schemes are related to different manufacturing conditions of PMMA (anionic or free radical polymerization process, the latter resulting in saturated end-groups, and/or presence of air leading to peroxide formation) [39,43,44]. The presence of sulfur, oxygen and nitrogen (see Section 2.1) may also be responsible for the occurrence of weak-bond cleavage at low temperatures.

In the case of PE, pyrolysis occurred in one stage between 340 and 500 °C, with a negligible residual solid yield of 0.5 wt% [7,45–47]. Although this polymer has a simple chemical structure, many discrepancies related to its decomposition have been reported [6]; and a determination of its essential thermal characteristics is needed.

The PET, containing a glass filler, exhibited a single degradation step mainly through cleavage of ester bonds [48–50] between 336 and 550 °C, which follows the general trends observed in previous studies [51–54]. The resulting char yield (*ca.* 51.8 wt%) when compared to residue (*ca.* 10 wt%) obtained for pure PET [51] suggests that the presence of glass promotes secondary char-forming reactions at high temperatures [50], a phenomenon well documented in coal pyrolysis [29]. The pyrolysis of natural polymers requires more degradation stages and these occur in a broader temperature range. As exemplified in Figure 3, this is due to their chemical heterogeneity which results in a much larger number of parallel and consecutive bond-breaking reactions. After the dehydration stage, three major decomposition steps were observed for coal: *ca.* 2% weight loss between 134 and 277 °C with a maximum decomposition rate of 0.3 %/min, followed by *ca.* 27% loss (277-667 °C, 1.8 %/min) and then a slower degradation stage above 667 °C (0.8%/min). This pattern corresponds to the usual description of primary coal pyrolysis with the combination of fragmentation and crosslinking events leading to the escape of volatiles (both tar and non-condensables) and the formation of char, respectively [52]. The high char yield (56 wt%) for this sub-bituminous coal is within the expected range because of its relatively low H/C ratio and despite its relatively high O/C ratio [53].

Thermal decomposition of pine is typical for that of biomass in general [30]: it started earlier than that of coal and is normally related to decomposition of hemicelluloses. The fastest decomposition rate is much higher than for coal and is mainly due to cellulose decomposition. The final slow degradation stage is attributed to the decomposition of lignin. In terms of more detailed chemical events accompanying biomass pyrolysis, these are now better understood [30,54,55] and are consistent with its higher heteroatom content (especially O) than in the case of coals (Table 1 and Figure 3): the least stable functional groups produce volatiles through rearrangements or cracking reactions of molecules between 25 and 110 °C with a 7% weight loss, followed by successive and fast depolymerization of hemicelluloses (171-349 °C, 6.8 wt%/min) and cellulose (349-413, 10.2%/min) and the slow conversion of lignin (>413 °C, 0.8 wt/min). These decomposition stages are responsible for the main weight loss, 82.5%, and are in competition with the carbonization process in which benzene rings are rearranged to form a complex polycyclic matrix. The latter was reported to be promoted by the presence of oxygen resulting in the formation of heavy molecules at high temperatures through crosslinking reactions [30].

3.2 Pyrolysis kinetics and thermodynamics

Independently of the polymer type, it is well accepted that an increase in heating rate results in a shift of mass loss to higher temperatures; this can be due to an experimental artifact, thermal lag [12], mass transfer limitations and/or a chemical effect (thermal energy accumulation required for bond breaking) [56]. It is not surprising, therefore, that the investigation of heating rate effect has been the object of numerous controversies. There is no question that the product distribution depends on the temperature-time history of the devolatilizing polymer [57], but the effects on kinetics are still controversial [11]. In a study using multi-heating-rate procedures, it is particularly important to minimize experimental inaccuracies associated with thermal lag or estimation of kinetic parameters [11,12,14,28]. Here this has been pursued by selecting conditions for which the Biot number was less than 0.1 [12] which allowed us to operate in a chemically controlled regime (see TS1 for individual Biot number values).

Figure 4 shows the DTG and TGA curves obtained when the heating rate is increased by one order of magnitude. A shift of the maximum degradation temperature toward higher temperatures and wider temperature ranges was observed in the decomposition of each polymer, as expected [56]. This trend was also correlated with an increased weight loss rate (see Table S2 in Supplementary Information). Thus, for example, the maximum rate was doubled when the heating rate was doubled in each case, confirming an Arrhenius-type dependence of the pyrolysis process on temperature.

The usefulness of the differential method of Friedman based on the examination of Arrhenius plots (see Figure S1) has been well established as a simple yet powerful tool that provides mechanistic insights into the thermal degradation process [15,28]. Our results at the 95% confidence level are presented in Figure 5 and Table 3. The activation energy was found to gradually increase in all cases. The steep rise at high conversion (beyond 60 and 80%) for coal and pine is inevitably associated with a higher standard error; remarkably, a contrasting trend was displayed by the synthetic polymers, especially PMMA. The different pyrolysis stages for each polymer (Table 3) are obtained from these graphs and they can be used to quantify more precisely the thermal behavior of polymers. The physical significance of thus determined activation energy values has been the subject of some concern [58], and the relevant issues have been rationalized and addressed by a number of researchers [59,60]. Suffice it to point out that carefully conducted experiments lead to Eα values that represent a mean of individual energy barriers for many (mostly parallel) pyrolysis reactions [15,16]. Even when samples are carefully prepared and the operating conditions are rigorously controlled [14,28,61], it is notable that standard deviations vary to a large extent according to the type of polymer studied. By minimizing temperature gradients within the particles (for Biot number values less than 0.1), error bars may be considered as an accurate representation of spatial and temporal deviations linked to mean values of Eα. Larger variations observed for natural polymers are thus interpreted as a direct manifestation of their complex chemical nature and the variability of their constituent chemical bonds. For example, spatial heterogeneity is best expressed as the coefficient of variability (CV=σ/μ, where σ is the standard deviation and μ the mean). Its values for the polymers studied here (Table 3) increase with chemical complexity (Figure 3) in the following order: $CV_{PE} = 4\% < CV_{PMMA} = 7\% < CV_{PET} = 8\% < CV_{coal} = 18\% < CV_{pine} = 25\%$.

Such Eα variability can be exploited to assess the thermal behavior of polymers and underpin some molecular-scale events. As mentioned above, it reflects process complexity: in natural polymers, coal in particular, pyrolysis involves a wider range of reaction types than the typical ones present in pyrolysis of synthetic polymers (random scission, backbiting and unzipping). For example, the characteristic Eα increment for natural polymers at high conversion is also observed (albeit to a lesser extent) in PET pyrolysis; this trend coincides with the relatively high yield of char obtained in these cases (coal, pine and PET) and with the aromatic character of these polymers (Table 2 and

Figure 3). Effectively, Carrier *et al.* [28] ascribed this trend to the formation of an “aromatic polycyclic structure of a higher thermal stability” in pyrolysis of technical bio-polymers. In this context, Sonoyama and Hayashi [62] also observed an increasing tendency of apparent activation energy during the pyrolysis of coal and biomass and reported a “transition to forming char” at 200–250 kJ/mol, which is consistent with our results (Table 3).

By analogy with the pyrolysis of simple alkanes [63,64], the pyrolysis of the most stereo-regular polymer, PMMA, occurs in two stages, initial one at *ca.*170 kJ/mol for $0.06 < \alpha < 0.15$, followed by a second stage at *ca.* 202 kJ/mol (Table 3). This differs to a large extent from observations reported in the literature. Thus, for example, lower $E\alpha$ values, between 60 [18] and 77 kJ/mol [65], have been reported for the initial stage and ascribed to the dominant occurrence of unzipping reactions; subsequently, $E\alpha$ increased to 190 kJ/mol, decreased again to 60 kJ/mol and finally reached 230 kJ/mol [18]. These changes were attributed to alternations between unzipping and random scission degradation modes as a consequence of structural differences of PMMA prepared using a free radical or anionic method [39] and of resulting differences in molecular weight [38]. According to Holland *et al.* [39] and the trends reported here (Figure 5c), the PMMA used has been prepared by anionic polymerization: it is characterized by an abundance of saturated end-groups and hence by its higher thermal stability [66]. Therefore the dominant reaction here is random chain initiation, where C-C bonds are broken to trigger the depolymerization process [66]. Indeed, Arisawa *et al.* [66] have reported 180-276 kJ/mol as the apparent activation energy range for monomer (MMA) evolution (and 188-272 kJ/mol for the whole process) during flash pyrolysis of anionically polymerized PMMA with different MWs; similarly, Manring [67] obtained an activation energy of 262 kJ/mol for saturated PMMA, whose degradation was characterized as “random initiation followed by complete depolymerisation of the polymer chain”. The discrepancies are thought to be due to MW differences: the energy barrier is indeed expected to increase with MW [38,66,67]. It is worth noting that PMMA has been selected in this study as an emblematic case where a maximum monomer yield can be achieved. (Indeed, Kaminsky and Franck obtained >97 wt% monomer yield [40].) This results from steric hindrance of intramolecular hydrogen transfer, which in turn favors unzipping reactions [68].

In the case of PE, the global activation energy increases initially from 177 to 194 kJ/mol between 0.06 and 0.13 to finally display a decreasing trend between 203 and 173 kJ/mol for $\alpha > 0.13$ (Figure 5e). The resulting average value of 187 kJ/mol over the whole conversion range is inferior to values reported in a recent compilation on LDPE kinetics [69]; and therefore suggests that discrepancies in the prediction of apparent kinetic parameters are difficult to avoid because of the extensive choice of techniques and approaches. In an attempt to fill the ‘gaps’ in mechanistic understanding [6], a number of researchers have considered every individual chemical reaction leading to PE degradation [6,70–73]. Thus, for example, Levine and Broadbelt presented a detailed model with 11,000 reactions and 151 different species [70] including a theoretical value of 375 kJ/mol for chain scission. Despite such contradictions in the literature, a common degradation pattern for PE pyrolysis has emerged. The major monomer formation pathway is often identified as ‘unzipping’ (β-scission of a chain-end radical), while backbiting and random-chain scissions mainly result in the production of both monomers and oligomers. On the other hand, cross-linking reactions allow the creation of bonds between two adjacent polymer chains promoting the formation of oligomers.

The case of PET is also emblematic; due to its ubiquitous commercial use, the kinetics of its depolymerization has been intensively studied. Its highly oxygenated nature (Figure 3 and Table 1) is responsible for straightforward degradation pathways, in one stage (Figure 5 and Table 3) through C-O and Ar-C bond breaking with the consequent release of CO_2, benzoic acid and/or benzene [74]. As mentioned in Section 3.1, the char yield is substantial, 51.8 wt.%; it is attributed to the low cleavage propensity of C-C bonds within the main chain in the range of 300-600 °C [75], but may also be due to the presence of inorganic fillers (*e.g.*, glass) that promotes aromatic condensation reaction [44]. During the first stage (Figures 4d and 5d) at <80% conversion, with an apparent activation energy of 193 kJ/mol, PET decomposes mainly by β-H transfer reactions, where hydrogen atoms in β position are transferred to a more stable carbon with subsequent scission of the molecule; rearrangement reactions leading to formation of new ester links and decarboxylation reactions (CO_2 evolution) occur as well to obtain the major products, benzoic acid and vinyl terephthalate [76]. The increasing apparent activation energy above 80% conversion (Table 3 and Figure 5d) is signature of char formation [77,78], as mentioned above.

Natural polymers display more irregular thermogravimetric curves with more degradation stages and a higher degree of heterogeneity (Figure 4 and Table 2). Although detailed mechanistic interpretations are difficult (in the absence of product evolution analyses), it is obvious that coal is less reactive than both the biomass and the three synthetic polymers. The large initial energy barrier (*ca.* 200 kJ/mol) is attributed not only to the relatively facile decarboxylation and cleavage of weak bonds between the aromatic structural units (see arrows in Figure 3a) but also to alkylation [79]. The second stage (Table 3) corresponds mainly to tar evolution, *ca.* 241 kJ/mol, which is close to the mean activation energy (230 kJ/mol) that Solomon *et al.* [52] attributed to this process; and the third stage, with an increasing activation energy (252-356 kJ/mol), corresponds to the repolymerization and condensation processes, where the abundant crosslinking reactions are important. These results are analogous to those obtained in coal liquefaction [80] as well as those of Golikeri and Luss [81], according to which the overall activation energy varies with the degree of conversion and therefore complex molecule reactivity should be analyzed according to groups of reactions with similar energy barriers.

The higher reactivity of biomass is a consequence of the presence of abundant oxygen (>25% in the polysaccharide and substituted polyphenol structures of cellulose and lignin; see Table 1). Its content depends on relative amount of lignin, cellulose and hemicelluloses, which in turn decompose over different temperature ranges [82]. The two stages of pine pyrolysis are clearly distinguishable: (i) for α=0.06-0.8 fragmentation of hemicelluloses, cellulose and lignin occurs [83,84], whose respective energy barriers of 55-187, 195-236 and 35-267 kJ/mol had been determined [28]; and (ii) between α=0.81-0.91, whose high energy barrier is due to the formation of a complex polycyclic aromatic structure (char formation) [28,84]. It should be noted that thermal decomposition of lignin occurs during the entire process, especially at high temperatures, which demonstrates the wide variety of bonds in its structure [28,83]. Similar to the results reported here, Yao *et al.* [85] obtained, using Friedman’s method, a mean activation energy of 161.5±3 kJ/mol at 0.1 < α < 0.6 for pine pyrolysis, and Kim *et al*. [84] reported an activation energy between 145 and 302 kJ/mol that also depended on conversion.

3.3 Structure-reactivity relationship

A much improved understanding of the kinetics of polymer pyrolysis can be achieved, in principle, by establishing a relationship with relevant thermodynamic parameters based on the venerable Evans-Polanyi approach [86]. This approach has been found particularly useful to assess the homolytic character of bond scission for polyethylene [70], polypropylene [87], polystyrene, polybutadiene and polyisoprene [88] for which strong linear relationships were obtained. In an attempt to apply this approach here, we used the classical group additivity method to determine the reaction enthalpies of relevant pyrolysis initiation reactions, *i.e.*, those leading to the initial thermal breakdown of the polymers (see Table S3). The results are summarized in Table 4. Products were defined according to bond stability and previously discussed mechanistic considerations. For synthetic polymers, and PMMA in particular, dissociation of C-C bonds located at both the extreme of the chain (end-chain scission) and at any other point in the chain (random scission) have been taken into account. In the case of PET, we considered homolytic scission of the C-O bond [77,78,89,90]. The enthalpies that characterize biomass pyrolysis were evaluated by taking into account its lignocellulosic character and the primary depolymerization stages that occur through the rupture of main covalent bonds between monomers. For coal, which displays more complex degradation patterns, the selection of main primary pyrolysis reactions has been done according to the classification proposed by Solomon [52]. The various weak bonds within the coal structure, where depolymerization starts, are indicated in Figure 3a.

Reaction enthalpies related to synthetic polymers pyrolysis vary little, between 342 and 347 for PMMA and between 311 and 351 kJ/mol for PET; in contrast, those for natural polymers vary over a large range, between 222 and 336 kJ/mol for coal and 220 and 454 kJ/mol for pine (Table 4). This observation reflects the chemical bond heterogeneity within natural polymers. In particular, the highest value of 454 kJ/mol obtained for the β-1,4 (3) glycosidic bond breakdown is attributed to the presence of ester groups (Figure 3) providing additional resonance stabilization to the radical intermediates. It is important to note here that the selection of homolysis reactions for natural polymers is at variance with recent findings. The cleavage of gycosidic bonds in cellulose, for example, occurs by concerted reactions (224 kJ/mol) rather than by a simple free-radical process (353 kJ/mol).[91,92]

The values calculated for PMMA, pine and coal are in agreement with the literature. For example, Stoliarov *et al*. (2003) [93] obtained an enthalpy of reaction of 358 kJ/mol for end-chain initiation scission of a PMMA molecule with saturated end (*vs.* 342 kJ/mol obtained here) employing reactive molecular dynamics. In the case of biomass, the average enthalpy remains in the range generally assumed for the primary biomass pyrolysis stage [94]. The values calculated for coal (between 222 and 336 kJ/mol) are within the ranges defined by Shi *et al.* [79] between 150 and 430 kJ/mol for typical bonds (linkage between $C_{aromatic}$ or $C_{aliphatic}$ with $C_{aliphatic}$, $C_{aromatic}$, O, N or S and S-S bond). Although establishing such correspondences does validate our approach (*i.e.*, appropriate selection of initiation reactions and acceptable accuracy using Benson's group additivity method), its simplifying assumptions should be noted (*e.g.*, strong bonding between polymers, in the case of pine, and between PET chains was not considered).

Table S3 contains the details of the procedure used to obtain the values shown in Table 4. The reaction enthalpy of process initiation was determined by taking a simple average of calculated enthalpies; only in the case of pine was the enthalpy of reaction calculated based on a combination of individual enthalpies for hemicelluloses, cellulose and lignin based on their mass ratios within the original biomass [20], resulting in a weighted average reaction enthalpy of 321 kJ/mol.

When selecting the type of reaction to model the primary stage of pyrolysis, we have made the assumption that depolymerization of both synthetic and natural polymers begins at weakest links in their structure. The experimentally derived energy barriers (see Section 3.2) are combined in Figure 6 with the above described thermodynamic parameters, as a test of this commonly adopted hypothesis. For the sake of robustness, previous datasets for biopolymers, α-celllose and lignin [28], were added. The existence of a commonly reported trend is confirmed, but the correlation ($R^2 = 0.25$) is weak for this limited data set. Formation of first radicals by initiation reactions is therefore not necessarily the rate-determining step; and pyrolysis reactions not only include both atom and electron transfer, as well as polar effects [95], but also reflect important bond-strength and structural differences between reactants and products, including kinetically important transition-state stabilization due to aromatic resonance [96–98]. And its implications are instructive, especially when considering the deviation of the slope (0.25 ± 0.20) from the value of 1.0 for homolytic dissociation [88,99], which emphasizes the fundamental differences existing within pyrolysis modes (e.g., ionic and non-ionic modes) of polymers.

When the slope is near 0.5, the transition-state is neither reactant-like nor product-like [99]. Whether the positive value of the intercept (95.5 ± 63.4) has physical meaning or is an artifact of the data scatter is an issue that should be explored in further studies.

5. Summary and Conclusions

The pyrolysis kinetics of representative natural and synthetic polymers were compared in an attempt to contribute to a more rational design of their degradation processes. Both the global activation energies and the dissociation energies of their principal weak bonds were determined using well established methodologies. The applicability of the Evans-Polanyi principle was then explored to rationalize the similarities and differences in their pyrolysis mechanisms.

Decomposition of synthetic polymers reached higher rates than that of natural polymers and occurred over a narrower temperature range. Synthetic polymers decomposed in two steps; natural polymers decomposed in two or more steps and produced a higher char yield. The abundant solid residue obtained in the special case of PET is tentatively attributed to the catalytic effect of inorganic impurities.

Polymer reactivity was quantified by determining the temporal evolution of activation energies using Friedman’s isoconversional method. A good linear correlation of relevant data confirmed the convenience of calculating the global activation energy as a function of conversion. This procedure revealed that the pyrolysis of natural polymers was more complex than that of synthetic polymers. These results are consistent with the intuitive expectation that pyrolysis proceeds in the order of increasing bond strength; indeed, in the simple case of PMMA the gradual activation energy increase is in agreement with the fact that the weakest bonds are cleaved first, and higher temperature or longer times are necessary for the stronger bonds to break. This trend suggests that weak bond scission represents the rate-limiting radical generation step in the pyrolysis process. In the case of natural polymers, global activation energy values at low conversion levels represent the scission of a much wider variety of bonds of varying strengths, which are further modulated through stereoelectronic effects. Indeed, this heterogeneity was reflected in the spatial variability coefficient (CV) of their activation energies. The trend of increasing activation energy at the end of PET pyrolysis, as well as that observed for coal and pine, is attributed to the char-forming aromatization process.

Differences and similarities in the structure-reactivity relationship for the various polymers were explored by combining these kinetic results with calculations of enthalpies for homolytic scission of representative weak bonds. Benson's group contribution method revealed the same chemical structure hierarchy between natural and synthetic polymers. Upon applying the Evans-Polanyi principle we obtained only a modest positive correlation between global activation energy and weak-bond dissociation energy. Additional steps subsequent to the formation of first radicals are thus kinetically significant, and accounting for spatial variability of bond cleavage processes among the different polymers remains a challenge. But as we pursue a practical model for recycling of organic waste materials, we expect that increasingly reliable kinetic parameters will be obtained using the proposed intermediate approach which avoids the excessive simplicity of the ubiquitious first-order kinetics as well as the excessive complexity (and mathematical intractability) of detailed mechanistic schemes.

ACKNOWLEDGMENTS

We gratefully acknowledge the financial support of projects INNOVA Chile 13IDL2-18714 and FONDECYT 1120609, as well as insightful reviewers' comments that have improved the clarity of our conclusions.

References

[1] Plastics Europe, Plastics - the Facts 2015, 2015. doi:10.1016/j.marpolbul.2013.01.015.

[2] The Scrap Recycling Industry: Plastics, Inst. Scrap Recycl. Ind. Inc. (2013) 2013.

[3] Plastic Waste Management Institute, PWMI Newsletter, (2013).

[4] R.C. Thompson, C.J. Moore, F.S. vom Saal, S.H. Swan, Plastics, the environment and human health: current consensus and future trends., Philos. Trans. R. Soc. Lond. B. Biol. Sci. 364 (2009) 2153–2166. doi:10.1098/rstb.2009.0053.

[5] S.M. Al-Salem, P. Lettieri, J. Baeyens, Recycling and recovery routes of plastic solid waste (PSW): a review., Waste Manag. 29 (2009) 2625–2643. doi:10.1016/j.wasman.2009.06.004.

[6] M.L. Poutsma, Reexamination of the Pyrolysis of Polyethylene : Data Needs , Free-Radical Mechanistic Considerations , and Thermochemical Kinetic Simulation of Initial Product-Forming Pathways, Macromolecules. 36 (2003) 8931–8957.

[7] P. Kannan, S. Ibrahim, K. Suresh Kumar Reddy, A. Al Shoaibi, C. Srinivasakannan, A Comparative Analysis of the Kinetic Experiments in Polyethylene Pyrolysis, J. Energy Resour. Technol. 136 (2014) 24001-1–6. doi:10.1115/1.4025595.

[8] M.L. Poutsma, Mechanistic analysis and thermochemical kinetic simulation of the pathways for volatile product formation from pyrolysis of polystyrene, especially for the dimer, Polym. Degrad. Stab. 91 (2006) 2979–3009. doi:10.1016/j.polymdegradstab.2006.08.015.

[9] M.L. Poutsma, Comparison of literature models for volatile product formation from the pyrolysis of polyisobutylene at mild conditions: Data analysis, free-radical mechanistic considerations, and simulation of initial product-forming pathways, J. Anal. Appl. Pyrolysis. 73 (2005) 159–203. doi:10.1016/j.jaap.2005.02.009.

[10] C. Di Blasi, Modeling chemical and physical processes of wood and biomass pyrolysis, Prog. Energy Combust. Sci. 34 (2008) 47–90. doi:10.1016/j.pecs.2006.12.001.

[11] J.E. White, W.J. Catallo, B.L. Legendre, Biomass pyrolysis kinetics: A comparative critical review with relevant agricultural residue case studies, J. Anal. Appl. Pyrolysis. 91 (2011) 1–33.

[12] J. Lédé, O. Authier, Temperature and heating rate of solid particles undergoing a thermal decomposition. Which criteria for characterizing fast pyrolysis?, J. Anal. Appl. Pyrolysis. 113 (2015) 1–14. doi:10.1016/j.jaap.2014.11.013.

[13] M. Gronli, M.J. Antal, G. Várhegyi, A Round-Robin Study of Cellulose Pyrolysis Kinetics by Thermogravimetry, Ind. Eng. Chem. Res. 38 (1999) 2238–2244. doi:10.1021/ie980601n.

[14] S. Vyazovkin, A.K. Burnham, J.M. Criado, L.A. Pérez-maqueda, C. Popescu, N. Sbirrazzuoli, ICTAC Kinetics Committee recommendations for performing kinetic computations on thermal analysis data, Thermochim. Acta. 520 (2011) 1–19. doi:10.1016/j.tca.2011.03.034.

[15] S. Vyazovkin, N. Sbirrazzuoli, Isoconversional kinetic analysis of thermally stimulated processes in polymers, Macromol. Rapid Commun. 27 (2006) 1515–1532. doi:10.1002/marc.200600404.

[16] S. Vyazovkin, Model-free kinetics Staying free of multiplying entities without necessity, J. Therm. Anal. Calorim. 83 (2006) 45–51.

[17] H.L. Friedman, Kinetics of thermal degradation of char-forming plastics from thermogravimetry. Application to a phenolic plastic, J. Polym. Sci. Part C Polym. Symp. 6 (1964) 183–195. doi:10.1002/polc.5070060121.

[18] J.D. Peterson, S. Vyazovkin, C.A. Wight, Stabilizing effect of oxygen on thermal degradation of poly(methyl methacrylate), J. Phys. Chem. B. 103 (1999) 8087–8092. doi:10.1002/(SICI)1521-3927(19990901)20:9<480::AID-MARC480>3.0.CO;2-7.

[19] P.A. Willems, G.F. Froment, Kinetic modeling of the thermal cracking of hydrocarbons. 1. Calculation of frecuency factors, Ind. Eng. Chem. Res. 27 (1988) 1959–1966. doi:10.1021/ie00083a002.

[20] A. Moore, S. Park, C. Segura, M. Carrier, Fast pyrolysis of lignin-coated radiata pine, J. Anal. Appl. Pyrolysis. 115 (2015) 203–213. doi:10.1016/j.jaap.2015.07.017.

[21] E. Cetin, R. Gupta, B. Moghtaderi, Effect of pyrolysis pressure and heating rate on radiata pine char structure and apparent gasification reactivity, Fuel. 84 (2005) 1328–1334. doi:10.1016/j.fuel.2004.07.016.

[22] S. Krerkkaiwan, C. Fushimi, A. Tsutsumi, P. Kuchonthara, Synergetic effect during co-pyrolysis/gasification of biomass and sub-bituminous coal, Fuel Process. Technol. 115 (2013) 11–18. doi:10.1016/j.fuproc.2013.03.044.

[23] P. Nowicki, R. Pietrzak, Effect of ammoxidation of activated carbons obtained from sub-bituminous coal on their NO2 sorption capacity under dry conditions, Chem. Eng. J. 166 (2011) 1039–1043. doi:10.1016/j.cej.2010.11.101.

[24] E.I. Kauppinen, T.A. Pakkanen, Coal Combustion Aerosols: A Field Study, Environ. Sci. Technol. 24 (1990) 1811–1818.

[25] C.L. Senior, L.E. Bool, S. Srinivasachar, B.R. Pease, K. Porle, Pilot scale study of trace element vaporization and condensation during combustion of a pulverized sub-bituminous coal, Fuel Process. Technol. 63 (2000) 149–165. doi:10.1016/S0378-3820(99)00094-6.

[26] J. Clayden, N. Geeves, S. Warren, Polimerization, in: Org. Chem., 2nd ed., Oxford University Press, 2012: p. 1234.

[27] A. Helin, H. Stryker, G. Mantell, Emulsion polymerization of ethylene I.

Polymerization Formulas and Conditions, 1Journal Appl. Polym. Sci. 9 (1965) 1797–1805.

[28] M. Carrier, L. Auret, A. Bridgwater, J.H. Knoetze, Using Apparent Activation Energy as a Reactivity Criterion for Biomass Pyrolysis, Energy & Fuels. 30 (2016) 7834–7841. doi:10.1021/acs.energyfuels.6b00794.

[29] A.W. Scaroni, M.R. Khan, E. Semih, L.R. Radovic, Coal Pyrolysis, in: Ullmann's Encycl. Ind. Chem., Sixth edit, Wiley-VCH Verlag GmbH & Co. KGaA, 2000: pp. 719–754.

[30] F.X. Collard, J. Blin, A review on pyrolysis of biomass constituents: Mechanisms and composition of the products obtained from the conversion of cellulose, hemicelluloses and lignin, Renew. Sustain. Energy Rev. 38 (2014) 594–608. doi:10.1016/j.rser.2014.06.013.

[31] S.W. Benson, J.H. Buss, Additivity Rules for the Estimation of Molecular properties. Thermodynamic Properties., J. Chem. Phys. 29 (1958) 546–572. doi:10.1007/s13398-014-0173-7.2.

[32] N. Cohen, S.W. Benson, Estimation of Heats of Formation of Organic-Compounds By Additivity Methods, Chem. Rev. 93 (1993) 2419–2438. doi:Times Cited: 328.

[33] J.T. Larrain Correa, Relación entre estructura y reactividad en la pirólisis de plásticos: una comparación con polímeros naturales, University of Concepción, 2016.

[34] E.S. Domalski, E.D. Hearing, Estimation of the Thermodynamic Properties of C-H-O-N-S-Halogen Compounds at 298.15 K, J. Phys. Chem. Ref. Data. 22 (1993) 805–1159.

[35] M.L. Poutsma, Fundamental reactions of free radicals relevant to pyrolysis reactions, J. Anal. Appl. Pyrolysis. 54 (2000) 5–35.

[36] A. Zakarian, Properties of atoms, radicals, and bonds, (n.d.). https://labs.chem.ucsb.edu/zakarian/armen/11---bonddissociationenergy.pdf.

[37] A. Barlowt, R.S. Lehrle, J.C. Robb, D. Sunderland, Polymethylmethacrylate Degradation Kinetics and Mechanisms in the Temperature Range 340 to 460°C, Polymer (Guildf). 8 (1967) 537–545.

[38] M. Ferriol, A. Gentilhomme, M. Cochez, N. Oget, J.L. Mieloszynski, Thermal degradation of poly(methyl methacrylate) (PMMA): Modelling of DTG and TG curves, Polym. Degrad. Stab. 79 (2003) 271–281. doi:10.1016/S0141-3910(02)00291-4.

[39] B.J. Holland, J.N. Hay, The effect of polymerisation conditions on the kinetics and mechanisms of thermal degradation of PMMA, Polym. Degrad. Stab. 77 (2002) 435–439. doi:10.1016/S0141-3910(02)00100-3.

[40] W. Kaminsky, J. Franck, Monomer recovery by pyrolysis of poly(methyl methacrylate) (PMMA), J. Anal. Appl. Pyrolysis. 19 (1991) 311–318.

[41] K. Smolders, J. Baeyens, Thermal degradation of PMMA in fluidised beds, Waste Manag. 24 (2004) 849–857. doi:10.1016/j.wasman.2004.06.002.

[42] B. Kang, S.G. Kim, J. Kim, Thermal degradation of poly(methyl methacrylate) polymers: Kinetics and recovery of monomers using a fluidized bed reactor, J. Anal. Appl. Pyrolysis. 81 (2008) 7–13. doi:10.1016/j.jaap.2007.07.001.

[43] T. Kashiwagi, A. Inaba, J.E. Brown, K. Hatada, T. Kitayama, E. Masuda, Effects of Weak Linkages on the Thermal and Oxidative Degradation of Poly(methyl methacrylates), Macromolecules. 19 (1986) 2160–2168. doi:10.1021/ma00162a010.

[44] Z. Gao, T. Kaneko, D. Hou, M. Nakada, Kinetics of thermal degradation of poly(methyl methacrylate) studied with the assistance of the fractional conversion at the maximum reaction rate, Polym. Degrad. Stab. 84 (2004) 399–403. doi:10.1016/j.polymdegradstab.2003.11.015.

[45] İ. Kayacan, Ö.M. Doğan, Pyrolysis of Low and High Density Polyethylene. Part I: Non-isothermal Pyrolysis Kinetics, Energy Sources, Part A Recover. Util. Environ. Eff. 30 (2008) 385–391. doi:10.1080/15567030701457079.

[46] A. Aboulkas, K. El, A. El Bouadili, Thermal degradation behaviors of polyethylene and polypropylene . Part I : Pyrolysis kinetics and mechanisms, Energy Convers. Manag. 51 (2010) 1363–1369. doi:10.1016/j.enconman.2009.12.017.

[47] B. Saha, A.K. Maiti, A.K. Ghoshal, Model-free method for isothermal and non-isothermal decomposition kinetics analysis of PET sample, Thermochim. Acta. 444 (2006) 46–52. doi:10.1016/j.tca.2006.02.018.

[48] M. Artetxe, G. Lopez, M. Amutio, G. Elordi, M. Olazar, J. Bilbao, Operating conditions for the pyrolysis of poly-(ethylene terephthalate) in a conical spouted-bed reactor, Ind. Eng. Chem. Res. 49 (2010) 2064–2069. doi:10.1021/ie900557c.

[49] A. Brems, J. Baeyens, J. Beerlandt, R. Dewil, Resources , Conservation and Recycling Thermogravimetric pyrolysis of waste polyethylene-terephthalate and polystyrene : A critical assessment of kinetics modelling, "Resources, Conserv. Recycl. 55 (2011) 772–781. doi:10.1016/j.resconrec.2011.03.003.

[50] T. Yoshioka, G. Grause, C. Eger, W. Kaminsky, A. Okuwaki, Pyrolysis of poly(ethylene terephthalate) in a fluidised bed plant, Polym. Degrad. Stab. 86 (2004) 499–504. doi:10.1016/j.polymdegradstab.2004.06.001.

[51] B.G. Girija, R.R.N. Sailaja, G. Madras, Thermal degradation and mechanical properties of PET blends, Polym. Degrad. Stab. 90 (2005) 147–153. doi:10.1016/j.polymdegradstab.2005.03.003.

[52] P.R. Solomon, M.A. Serio, E.M. Suuberg, Coal Pyrolysis : Experiments, Kinetic Rates and Mechanisms, Prog. Energy Combust. Sci. 18 (1992) 133–220.

[53] D.K. Park, S.D. Kim, S.H. Lee, J.G. Lee, Co-pyrolysis characteristics of sawdust and coal blend in TGA and a fixed bed reactor, Bioresour. Technol. 101 (2010) 6151–6156. doi:10.1016/j.biortech.2010.02.087.

[54] H.J. Park, Y.K. Park, J.S. Kim, Influence of reaction conditions and the char separation system on the production of bio-oil from radiata pine sawdust by fast pyrolysis, Fuel Process. Technol. 89 (2008) 797–802. doi:10.1016/j.fuproc.2008.01.003.

[55] F. Collard, M. Carrier, J. Gorgens, Fractionation of Lignocellulosic Material With Pyrolysis Processing, in: Biomass Fractionation Technol. a Lignocellul. Feed. Based Biorefinery, 2016: pp. 81–101. doi:http://dx.doi.org/10.1016/B978-0-12-802323-5.00004-9.

[56] H. Juntgen, K.H. Van Heek, An update of german non-isothermal coal pyrolysis work, Fuel Process. Technol. 2 (1979) 261–293. doi:10.1016/0378-3820(79)90018-3.

[57] B. Gui, Y. Qiao, D. Wan, S. Liu, Z. Han, H. Yao, Nascent tar formation during polyvinylchloride (PVC) pyrolysis, 34 (2013) 2321–2329.

[58] S. Vyazovkin, C.A. Wight, Kinetics in Solids, Annu. Rev. Phys. Chem. 48 (1997) 125–149. doi:10.1146/annurev.physchem.48.1.125.

[59] A. Caballero, J.A. Conesa, Mathematical considerations for nonisothermal kinetics in thermal decomposition, J. Anal. Appl. Pyrolysis. 73 (2005) 85–100. doi:10.1016/j.jaap.2004.12.003.

[60] S. Vyazovkin, N. Sbirrazzuoli, Confidence intervals for the activation energy estimated by few experiments, Anal. Chim. Acta. 355 (1997) 175–180. doi:10.1016/S0003-2670(97)00505-9.

[61] A.K. Burnham, L.N. Dinh, A comparison of isoconversional and model-fitting approaches to kinetic parameter estimation and application predictions, J. Therm. Anal. Calorim. 89 (2007) 479–490.

[62] N. Sonoyama, J. Hayashi, Characterisation of coal and biomass based on kinetic parameter distributions for pyrolysis, Fuel. 114 (2013) 206–215. doi:10.1016/j.fuel.2012.04.023.

[63] A. Kossiakoff, F.O. Rice, Thermal decomposition of hydrocarbons, resonance stabilization and isomerization of free radicals, J. Am. Chem. Soc. 65 (1943) 590–595.

[64] P. A. Willems, G.F. Froment, Kinetic modeling of the thermal cracking of hydrocarbons. 2. Calculation of activation energies, Ind. Eng. Chem. Res. 27 (1988) 1966–1971. doi:10.1021/ie00083a002.

[65] P.R.E.J. Cowley, M. W., The Photo-Degradation of Polymethylmethacrylate. II. Evaluation of Absolute Rate Constants for a Depolymerization Reaction, Proc. R. Soc. A. 211 (1952) 320. doi:10.1098/rspa.1952.0045.

[66] H. Arisawa, T.B. Brill, Kinetics and mechanisms of flash pyrolysis of poly(methyl methacrylate) (PMMA), Combust. Flame. 109 (1997) 415–426. doi:10.1016/S0010-2180(96)00190-3.

[67] L.E. Manring, Thermal Degradation of Saturated Poly(methyl methacrylate), Macromolecules. 21 (1988) 528–530.

[68] C.L. Beyler, M.M. Hirschler, Thermal Decomposition of Polymers, in: SFPE Handb. Fire Prot. Eng. 3rd Ed., 2005: pp. 110–131.

[69] P. Kannan, S. Ibrahim, K. Suresh Kumar Reddy, A. Al Shoaibi, C. Srinivasakannan, A Comparative Analysis of the Kinetic Experiments in Polyethylene Pyrolysis, J. Energy Resour. Technol. 136 (2014) 24001-1–6. doi:10.1115/1.4025595.

[70] S.E. Levine, L.J. Broadbelt, Detailed mechanistic modeling of high-density polyethylene pyrolysis : Low molecular weight product evolution, Polym. Degrad. Stab. 94 (2009) 810–822. doi:10.1016/j.polymdegradstab.2009.01.031.

[71] N.A. Sezgi, W.S. Cha, J.M. Smith, B.J. McCoy, Polyethylene Pyrolysis: Theory and Experiments for Molecular-Weight-Distribution Kinetics, Ind. Eng. Chem. Res. 37 (1998) 2582–2591. doi:10.1021/ie980106r.

[72] T. Faravelli, G. Bozzano, C. Scassa, M. Perego, S. Fabini, E. Ranzi, M. Dente, Gas product distribution from polyethylene pyrolysis, 52 (1999) 87–103.

[73] J.F. Mastral, C. Berrueco, J. Ceamanos, Modelling of the pyrolysis of high density polyethylene Product distribution in a fluidized bed reactor, 79 (2007) 313–322. doi:10.1016/j.jaap.2006.10.018.

[74] A. Brems, J. Baeyens, C. Vandecasteele, R. Dewil, Polymeric Cracking of Waste Polyethylene Terephthalate to Chemicals and Energy, J. Air Waste Manage. Assoc. 61 (2011) 721–731. doi:10.3155/1047-3289.61.7.721.

[75] I. Cit, A. Sinag, T. Yumak, S. Ucar, Z. Misirlioglu, M. Canel, Comparative pyrolysis of polyolefins (PP and LDPE) and PET, Polym. Bull. 64 (2010) 817–834. doi:10.1007/s00289-009-0225-x.

[76] A. Buekens, Introduction to feedstock recycling of plastics, in: Feed. Recycl. Pyrolysis Waste Plast., 2006: pp. 1–41.

[77] A. Al-Mulla, H.I. Shaban, Degradation kinetics of poly(ethylene terephthalate) and poly (methyl methacrylate) blends, Polym. Bull. 58 (2007) 893–902. doi:10.1007/s00289-006-0712-2.

[78] I. Martín-Gullón, E. Esperanza, R. Font, Kinetic model for the pyrolysis and combustion of poly-(ethylene terephthalate) (PET), J. Anal. Appl. Pyrolysis. 58–59 (2001) 635–650.

[79] L. Shi, Q. Liu, X. Guo, W. Wu, Z. Liu, Pyrolysis behavior and bonding information of coal — A TGA study, Fuel Process. Technol. 108 (2013) 125–132. doi:10.1016/j.fuproc.2012.06.023.

[80] D.C. Cronauer, Y.T. Shah, R.G. Ruberto, Kinetics of Thermal Liquefaction of Belle Ayr Subbituminous Coal, Ind. Eng. Chem. Process Des. Dev. 17 (1978) 281–288. doi:10.1021/i260067a013.

[81] S. V Gollkerl, D. Luss, Analysis of Activation Energy of Grouped Parallel Reactions, AIChE J. 18 (1972) 277–282.

[82] M. Carrier, A. Loppinet-Serani, D. Denux, J.-M. Lasnier, F. Ham-Pichavant, F. Cansell, C. Aymonier, Thermogravimetric analysis as a new method to determine the lignocellulosic composition of biomass, Biomass and Bioenergy. 35 (2011) 298–307. doi:10.1016/j.biombioe.2010.08.067.

[83] J. Cai, W. Wu, R. Liu, G.W. Huber, A distributed activation energy model for the pyrolysis of lignocellulosic biomass, Green Chem. 15 (2013) 1331–1340. doi:10.1039/c3gc36958g.

[84] S.S. Kim, J. Kim, Y.H. Park, Y.K. Park, Pyrolysis kinetics and decomposition characteristics of pine trees, Bioresour. Technol. 101 (2010) 9797–9802. doi:10.1016/j.biortech.2010.07.094.

[85] F. Yao, Q. Wu, Y. Lei, W. Guo, Y. Xu, Thermal decomposition kinetics of natural fibers: Activation energy with dynamic thermogravimetric analysis, Polym. Degrad. Stab. 93 (2008) 90–98. doi:10.1016/j.polymdegradstab.2007.10.012.

[86] M.G. Evans, M. Polanyi, Inertia and driving force of chemical reactions, Trans. Faraday Soc. 34 (1938) 11–24. doi:10.1039/tf9383400011.

[87] T.M. Kruse, H. Wong, L.J. Broadbelt, Mechanistic Modeling of Polymer Pyrolysis : Polypropylene, Macromolecules. 36 (2003) 9594–9607.

[88] R. Vinu, L.J. Broadbelt, Unraveling Reaction Pathways and Specifying Reaction Kinetics for Complex Systems, Annu. Rev. Chem. Biomol. Eng. 3 (2012) 29–54. doi:10.1146/annurev-chembioeng-062011-081108.

[89] M.E. Bednas, M. Day, R. Ho, R. Sander, D.M. Wiles, Combustion and Pyrolysis of Poly(ethylene Terephthalate). I. The Role of Flame Retardants on Products of Pyrolysis, J. Appl. Polym. Sci. 26 (1981) 277–289.

[90] G. Montaudo, C. Puglisi, F. Samperi, Primary thermal degradation mechanisms of PET and PBT, Polym. Degrad. Stab. 42 (1993) 13–28.

[91] R. Vinu, L.J. Broadbelt, A mechanistic model of fast pyrolysis of glucose-based carbohydrates to predict bio-oil composition, Energy Environ. Sci. (2012) 9808–9826. doi:10.1039/c2ee22784c.

[92] X. Zhou, M.W. Nolte, H.B. Mayes, B.H. Shanks, L.J. Broadbelt, Experimental and mechanistic modeling of fast pyrolysis of neat glucose-based carbohydrates. 1. Experiments and development of a detailed mechanistic model, Ind. Eng. Chem. Res. 53 (2014) 13274–13289. doi:10.1021/ie502259w.

[93] S.I. Stoliarov, P.R. Westmoreland, M.R. Nyden, G.P. Forney, A reactive molecular dynamics model of thermal decomposition in polymers: I. Poly(methyl methacrylate), Polymer (Guildf). 44 (2003) 883–894. doi:10.1016/S0032-3861(02)00761-9.

[94] A.M.C. Janse, R.W.J. Westerhout, W. Prins, Modelling of flash pyrolysis of a single

wood particle, Chem. Eng. Process. Process Intensif. 39 (2000) 239–252. doi:10.1016/S0255-2701(99)00092-6.

[95] B.P. Roberts, A.J. Steel, An Extended Form of the Evans-Polanyi Equation: a Simple Empirical Relationship, J. Chem. Soc. Perkin Trans. 2 (1994) 2155–2162.

[96] A.A. Zavitsas, Hydrogen abstractions by radicals . Different approaches to understanding factors controlling reactivity, J. Chem. Soc. Perkin Trans. 2 (1998) 499–502.

[97] A.A. Zavitsas, Energy barriers to chemical reactions. Why, how and how much? Non-arrhenius behavior in hydrogen abstractions by radicals, J. Am. Chem. Soc. 120 (1998) 6578–6586. doi:10.1021/ja973698y.

[98] M.G. Evans, The Activation Energies of Reactions involving conjugated systems, Trans. Faraday Soc. 35 (1939) 824–834.

[99] P.E. Savage, Mechanisms and kinetics models for hydrocarbon pyrolysis, J. Anal. Appl. Pyrolysis. 54 (2000) 109–126. doi:10.1016/S0165-2370(99)00084-4.

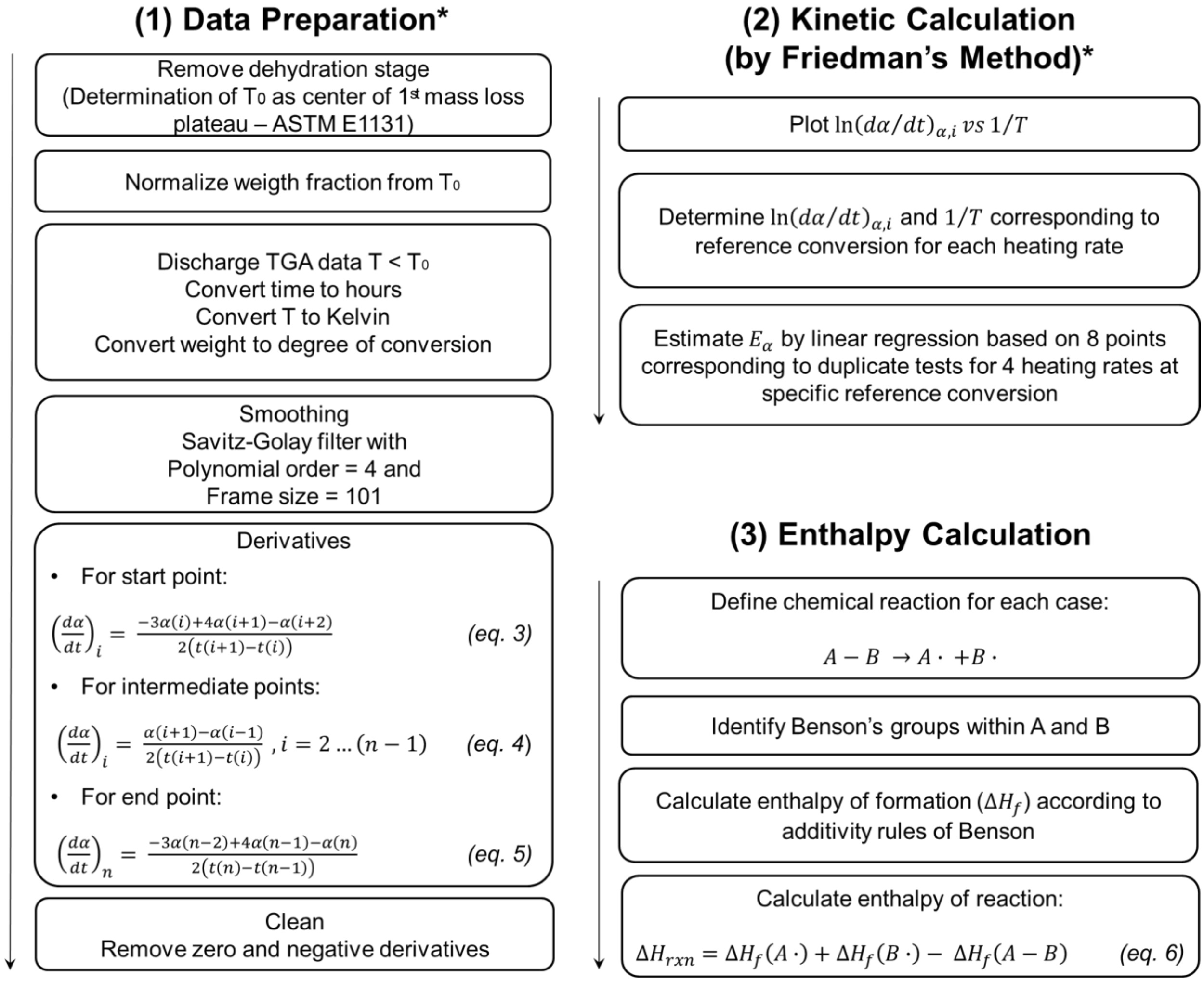

(1) Data Preparation*

Remove dehydration stage (Determination of T_0 as center of 1^{st} mass loss plateau – ASTM E1131)

Normalize weigth fraction from T_0

Discharge TGA data $T < T_0$
Convert time to hours
Convert T to Kelvin
Convert weight to degree of conversion

Smoothing
Savitz-Golay filter with
Polynomial order = 4 and
Frame size = 101

Derivatives

- For start point:

$$\left(\frac{d\alpha}{dt}\right)_i = \frac{-3\alpha(i)+4\alpha(i+1)-\alpha(i+2)}{2\big(t(i+1)-t(i)\big)} \quad \textit{(eq. 3)}$$

- For intermediate points:

$$\left(\frac{d\alpha}{dt}\right)_i = \frac{\alpha(i+1)-\alpha(i-1)}{2\big(t(i+1)-t(i)\big)}\ , i = 2 \ldots (n-1) \quad \textit{(eq. 4)}$$

- For end point:

$$\left(\frac{d\alpha}{dt}\right)_n = \frac{-3\alpha(n-2)+4\alpha(n-1)-\alpha(n)}{2\big(t(n)-t(n-1)\big)} \quad \textit{(eq. 5)}$$

Clean
Remove zero and negative derivatives

(2) Kinetic Calculation (by Friedman's Method)*

Plot $\ln(d\alpha/dt)_{\alpha,i}\ vs\ 1/T$

Determine $\ln(d\alpha/dt)_{\alpha,i}$ and $1/T$ corresponding to reference conversion for each heating rate

Estimate E_α by linear regression based on 8 points corresponding to duplicate tests for 4 heating rates at specific reference conversion

(3) Enthalpy Calculation

Define chemical reaction for each case:

$$A - B \ \rightarrow A\cdot\ + B\cdot$$

Identify Benson's groups within A and B

Calculate enthalpy of formation (ΔH_f) according to additivity rules of Benson

Calculate enthalpy of reaction:

$$\Delta H_{rxn} = \Delta H_f(A\cdot) + \Delta H_f(B\cdot) - \Delta H_f(A-B) \quad \textit{(eq. 6)}$$

*Adapted from [28]

Figure 1. Summary of methodology used.

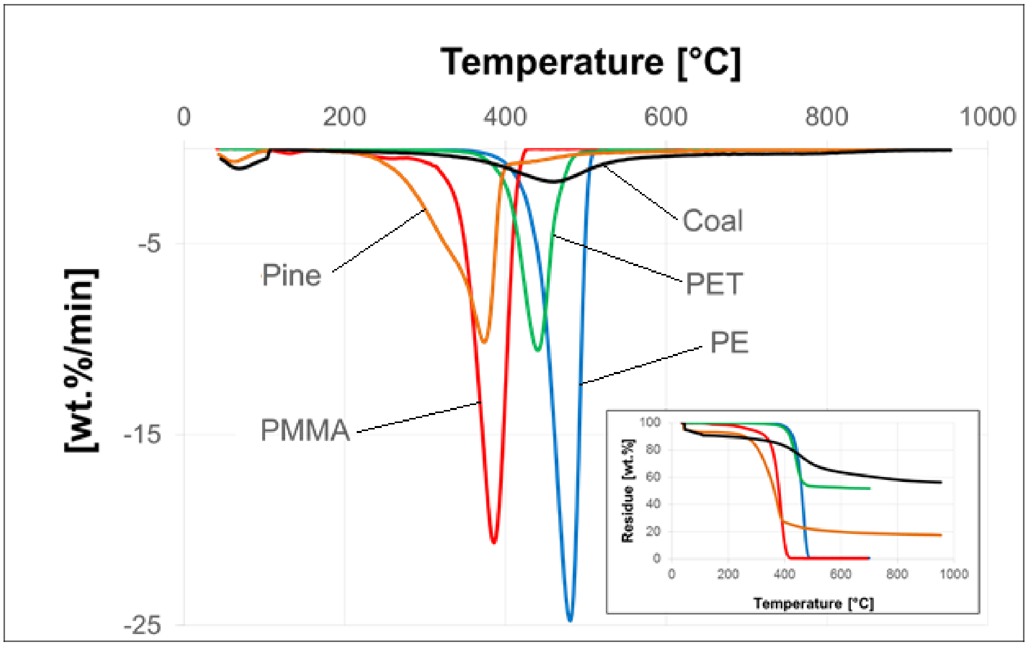

Figure 2. DTG and TGA curves for natural and synthetic polymers obtained at 10 °C/min in flowing N_2.

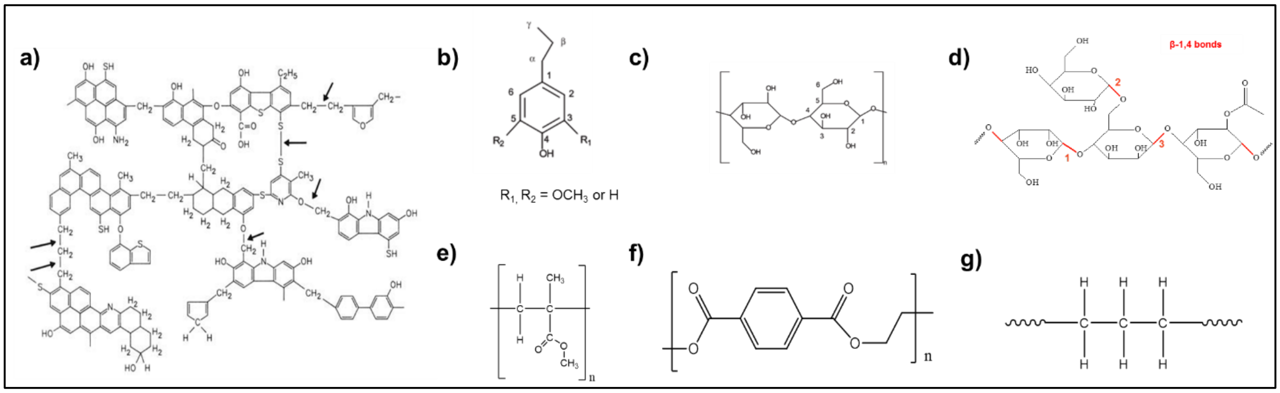

Figure 3. Chemical structure of polymers: (a) Wiser model of coal [29], the building units of lignin (b), cellulose (c) and hemicelluloses glucomannan (d) with a-d) adapted from [30]; and (e) PMMA, (f) PET and (g) PE.

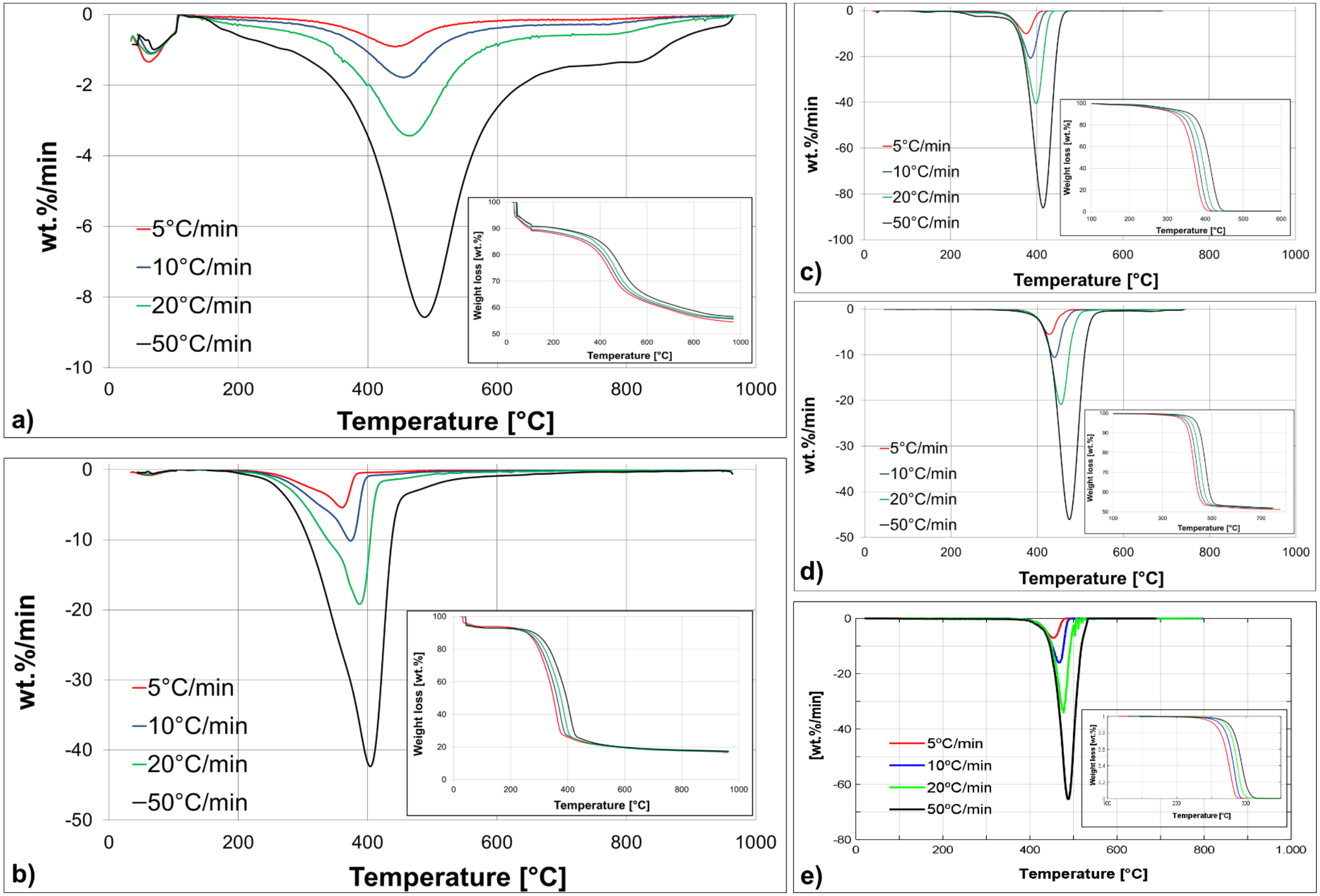

Figure 4. DTG and TGA curves at different heating rates for: a) coal, b) pine, c) PMMA, d) PET and e) PE (**Red**: 5°C/min, **Blue**: 10°C/min, **Green**: 20°C/min, **Black**: 50°C/min).

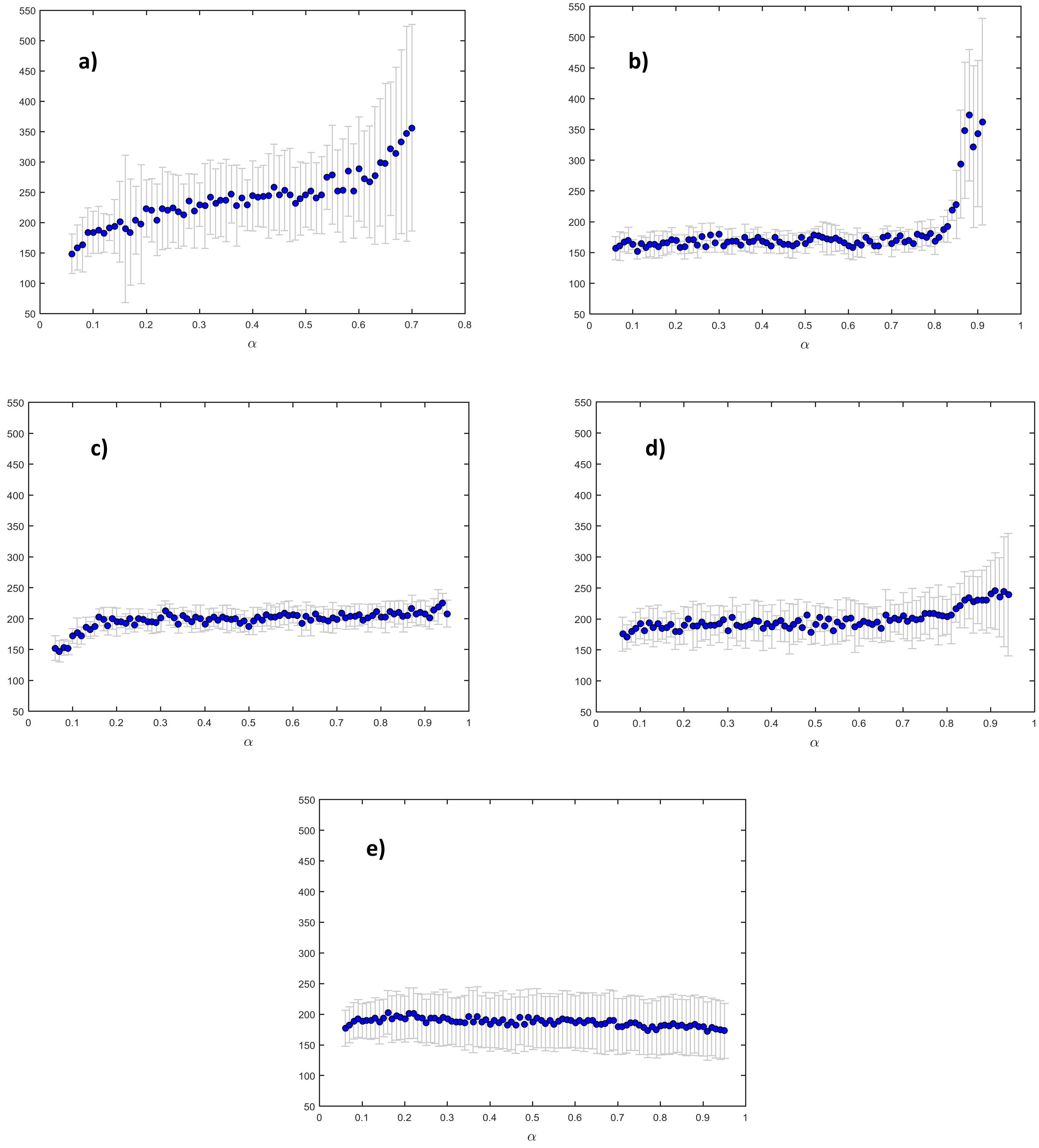

Figure 5. Mean activation energy (kJ/mol) *vs.* conversion (α) for natural and synthetic polymers with 95% confidence intervals: a) coal, b) pine, c) PMMA, d) PET and e) PE. Conversion increases from 0.05 to 0.95, except for coal and pine, where the linear correlation gives R^2 values below 0.9 for conversion values above 0.7 and 0.92, respectively. The grey bars represent the standard error at 95% confidence.

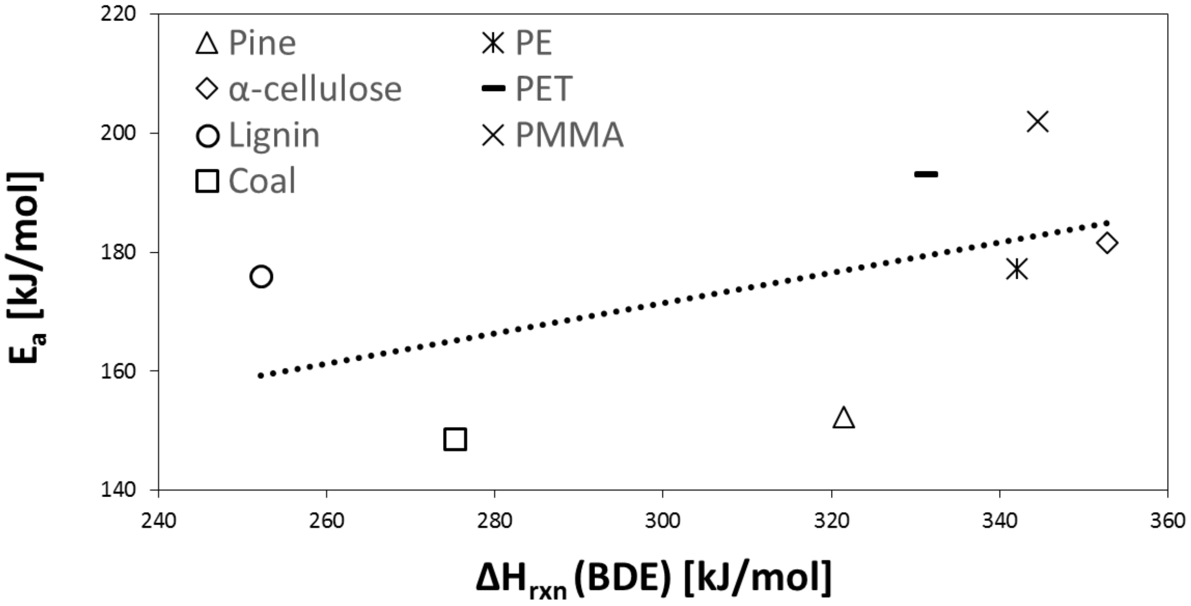

Figure 6. Evans-Polanyi relationship for pyrolysis of synthetic and natural polymers. The enthalpy values of weakest bond breakdown were added to Table S2 in Supplementary information.

Table 1. Elemental analysis of natural and synthetic polymers.

Polymer	**PMMA**	**PET**	**PE**	**Sub-bituminous coal**	**Pine**
C (%)[a]	61.2 ± 0.4	43.4 ± 0.4	84.4 ± 0.4	55.9 ± 0.2	49.7 ± 0.2
H (%)[a]	8.4 ± 0.2	3.2 ± 0.1	14.3 ± 0.1	6.4 ± 0.1	7.1 ± 0.1
N (%)[a]	0.6 ± 0.2	0.3 ± 0.0	n.d.	0.8 ± 0.1	0.5 ± 0.1
S (%)[a]	0.8 ± 0.0	n.d.	0.1 ± 0.0	0.3 ± 0.0	0.2 ± 0.0
O (%)[a,b]	28.8 ± 0.5	22.2 ± 0.7	1.2 ± 0.5	13.7 ± 0.6	41.8 ± 0.3
Ash (%)[a]	0.2 ± 0.0	30.9 ± 0.2	0.0 ± 0.0	23.1 ± 0.2	0.8 ± 0.0
Moisture (%)	1.6 ± 0.0	0.4 ± 0.0	0.2 ± 0.0	16.0 ± 0.1	9.2 ± 0.1
H/C ratio	1.66	0.88	2.03	1.36	1.72
O/C ratio	0.35	0.38	0.01	0.18	0.63

[a] dry basis; [b] O%=100-C%-H%-N%-S%-Ash%. n.d.: not detected.

Table 2. Summary of thermogravimetric data for selected natural and synthetic polymers.

Polymer type	Stage number	Decomposition temperature range (°C)*	Maximum decomposition temperature (ºC)	Rate of maximum decomposition (wt%/min)	Residue yield (wt%)
PMMA	1st	133 - 275	259	-0.56 ± 0.0	94.7 ± 0.3
	2nd	275 - 428	387	-21.1 ± 0.3	0.6 ± 0.1
PET	1st	336 - 550	441	-10.8 ± 0.3	51.8 ± 0.1
PE	1st	350 – 480	467	-26.1 ± 0.7	0.5 ± 0.5
Pine	1st	171-349	349	-6.8 ± 0.2	59.5 ± 0.8
	2nd	349-413	373	-10.2 ± 0.1	26.0 ± 0.2
	3rd	413	413	-0.8 ± 0.0	17.5 ± 0.2
Coal	1st	134-277	277	-0.3 ± 0.0	87.8 ± 1.0
	2nd	277-667	458	-1.8 ± 0.0	61.0 ± 0.8
	3rd	667	667	-0.3 ± 0.0	56.0 ± 0.4

Table 3. Mean activation energies at different levels of conversion for natural and synthetic polymers.

Polymer	**α range**	**Eα [kJ/mol]**	**Mean Eα [kJ/mol]**	**CV* [%]**
Coal	0.06-0.30	149-236	200 ± 22.9	18
	0.31-0.53	227-258	241 ± 8.0	
	0.54-0.70	252-356	292 ± 32.3	
Pine	0.06-0.80	152-182	168 ± 6.4	25
	0.81-0.91	175-373	277 ± 77.2	
PMMA	0.06-0.15	147-187	168 ± 15.5	6.7
	0.16-0.85	188-225	202 ± 6.8	
PET	0.06-0.79	171-209	193 ± 8.4	8.3
	0.80-0.94	204-245	229 ± 12.5	
PE	0.06-0.13	177-194	188 ± 5.5	3.5
	0.14-0.95	173-203	187 ± 6.6	

** Coefficient of variation*

Table 1. Enthalpy of reaction (bond dissociation energy) of the scission of principal bonds present in natural and synthetic polymers.

Polymer	**Bond type***	**ΔH_{rxn} [kJ/mol]**
Coal	PhCH$_2$-CH$_2$-CH$_2$Ph	307
	PhS-SPy	230
	PhO-CH$_2$Ph	222
	PyO-CH$_2$Ph	336
	FuCH$_2$-CH$_2$Ph	281
Lignin	α-O-4	220
	β-O-4	283
Cellulose	β-1,4	353
Hemicelluloses (glucomannan)	β-1,4 (1) and (2)	353
	β-1,4 (3)	454
PMMA	End-chain C-C bond	342
	Random C-C bond	347
PET	End-chain C-O bond	311
	Random C-O bond	351
PE	End-chain C-C bond	315
	Random C-C bond	368

* Ph: phenyl group; Py: pyridine group; Fu: furan group.